OPEN ACCESS

Saudi Journal of Civil Engineering
Abbreviated Key Title: Saudi J Civ Eng
ISSN 2523-2657 (Print) | ISSN 2523-2231 (Online)
Scholars Middle East Publishers, Dubai, United Arab Emirates
Journal homepage: https://saudijournals.com/journal/sjce/home

Original Research Article

Laboratory Evaluation of the Hydraulic Conductivity as a Function of Changes in the Particle Size of a Cubitermes Sp Termite Mound Soil Treated with Lime

Louis Ahouet[1,2,3*], Sylvain Ndinga Okina[1,2], Stiven Cardelin Marien Mangala,[1,2], E. P. Nkembo Mangue[2]

[1]Higher Institute of Architecture, Urbanism, Building and Public Works, Denis Sassou Nguesso University, Congo
[2]Higher National Polytechnic School (ENSP), Marien Ngouabi University – Brazzaville, Congo
[3]Control Office for Building and Public Works (BCBTP) – Brazzaville, BP 752, Congo

DOI: 10.36348/sjce.2024.v08i02.001 | **Received:** 23.12.2023 | **Accepted:** 29.01.2024 | **Published:** 01.02.2024

***Corresponding author:** Louis Ahouet
Higher Institute of Architecture, Urbanism, Building and Public Works, Denis Sassou Nguesso University, Congo

Abstract

This work characterizes the geotechnical properties and microstructure that served as a fundamental and more practical basis for describing the hydraulic conductivity of the lime-treated cubitermes sp termite mound soil. The results show that changes in particle size lead to a decrease in dry density and linear swelling. Permeability is strongly correlated with particle size distribution and compaction. Permeability increases up to the lime fixation point obtained at 6% of the lime content. Compaction for micropore reduction in treated soil is higher than in raw soil. The treated soil has a denser internal structure with agglomerations of dispersed clay particles. The increase in compaction energy reduces macropores and permeability, and the soil microstructure becomes homogeneous. Natural soil is highly impermeable, and soil-lime mixes are among the least draining materials. Higher values of hydraulic conductivity were obtained as a function of time. Soil and mixtures can be used in civil engineering works (earthworks). Correlations between hydraulic conductivity and particle size fractions are polylinear fits with R^2 (0.962-0.993) and the Slogistic1 model with χ^2($2.06E^{-15}$) for the mean silt fraction. This study is decisive for predicting hydraulic conductivity from the geotechnical properties of the soil, by solving the mathematical expressions of the models used.

Keywords: Hydraulic conductivity, Permeability, Cubitermes sp termite mound soil, Geotechnical.

1. INTRODUCTION

Dirt roads in the Republic of Congo account for around 86% of the total length of classified roads. Most of these roads are surfaced with lateritic gravel, natural gravel, silty sand or clay, etc [1]. However, the scarcity of road materials has led to the use of the cubitermes sp termite mound soil as an improvement layer for an earth road in the Plateau department, where it rains 9 months out of 12. Unfortunately, it has often been observed that earth roads deteriorate rapidly as soon as they are put into service, losing all or part of the wearing course under the combined action of traffic, rainfall and maintenance [1, 2]. The use of a material containing fine clay in the wearing layer requires special provisions because of its instability in the presence of water. The use of non-stabilized cubitermes sp termite mound soil as a wearing layer requires special arrangements (backfill, rain barrier, regular reprofiling and new soil inputs) because of its sensitivity to water, and losses of the fine fraction due to wind and run-off. These soils can be found as soon as they are extracted or as a result of bad weather conditions, to such an extent that machine traffic becomes difficult or even impossible, making them difficult to use [3, 4]. Given the importance of earth roads in the socio-economic life of the country, alternative solutions have been sought to increase their lifespan and thus guarantee the investments made. This involves the chemical stabilization of soils using hydraulic binders (lime, cement). For termite mound soils containing fine particles of very high clay content, lime is the ideal binder compared with cement for treating this soil. Soil-lime treatment is a tried and tested technique that has been perfectly developed for over twenty years [5]. The success of soil-lime treatment depends in particular on the texture, type and content of clay, the nature and content of lime, the curing time and the curing

temperature [6]. Lime makes the soil able to withstand site machinery traffic, depending on the water status of the soil at the time of construction. For the lime-improved wearing layer that will be exposed to rainwater, it is important to understand its behavior in the presence of water. In geotechnical engineering, hydraulic conductivity is an essential parameter for determining water transfer in the soil [7]. For the wearing layer of cubitermes sp termite mound soils treated with lime, permeability is an important factor to take into account when assessing the soil's resistance to moisture during the rainy season. However, the variation in the hydraulic conductivity of soils treated with binders remains difficult to explain due to the systematic lack of analysis of the coupling between soil permeability and microstructure [8, 9]. Several studies in the literature report that the incorporation of lime into the soil improves the geotechnical properties of the soil, which is reflected in the ease with which the material can be used and its compatibility. The effect of soil-binder treatment on soil hydraulic conductivity is the subject of ongoing debate. To our knowledge, the hydraulic conductivity of a fine soil treated with lime as a function of changes in particle size fractions has not yet been reported. It is important that the soil-binder combination be subjected to the necessary tests. The aim of this work is to evaluate in the laboratory the effect of lime treatment of the cubitermes sp termite mound soil on the saturated hydraulic conductivity of undisturbed soil samples. To do this, the geotechnical properties coupled with the microstructure will be determined on the one hand and, on the other, the relationships between the hydraulic conductivity and the geotechnical properties will be established.

2. MATERIAL AND METHODS

2.1 Material

The soil was sampled at coordinates 150 45' E and 20 29' S. The hydrated lime used was Pascal brand "CL 90-S", purchased on a local market. The cubitermes sp termite mounds are mushroom-shaped, with an average diameter of 30 cm and a height of 30 to 50 cm. Figure 1 shows soil samples from termite mounds, used for the construction of earth roads in the absence of conventional road materials.

Fig. 1: Cubitermes sp termite mound soil

The mushroom-shaped grey-black soil of the cubitermes sp termite mound, shown in Figure 1, is built by a species of termite. To build their nests, termites can look for soil more than 10 m deep. Termites saliva mixed with soil consolidates the latter by modifying its physical-mechanical properties, giving it new properties used in road geotechnics. Fig.2 shows an earth road in the Republic of Congo, covered with a 30 cm wearing layer of cubitermes sp termite mound soil.

Fig. 2: View of the earth road

Soil from cubitermes sp termite mounds is being used on a large scale for the construction of a 65 km-long earth road (Fig.2). The road, which is covered with soil from cubitermes sp termite mounds, is treated with lime to reduce dust and prevent water infiltration into the road structure. Some sections of this road have lasted from 3 to 5 years, depending on the level of traffic and the action of water on the road. It is an impermeable material, suitable for civil engineering works and very consistent, difficult to apply on site.

2.2 METHODS

Origin Pro 2019b software was used to develop correlations between the geotechnical properties of the soils. The mathematical model selected was the one with the highest coefficient of determination R^2 and the lowest Chi-square (χ^2). Chi-square (χ^2) is used to test the independence of two random variables. On the basis of the physical and chemical properties of the grains, cubitermes sp termite mound soil and soil-lime mixtures (3%, 5%, 6%, 7%, 9%) are classified according to AASHTO T88-70 [10], and USCS [11]. Figure 3 shows how the soil-lime mixture is mixed by hand in the laboratory after the termite mound soil has been crushed.

Fig. 3: The soil-lime mixture

Figure 3 explains that after crushing, the soil was sieved to retain only grains with a diameter of less than 2 mm. Soil-lime mixtures of 0% (natural soil), 3%, 5%, 6%, 7% and 9% by dry mass of sieved soil were prepared by carefully stirring the sieved soil and lime until the mixtures were homogeneous. The tests were then carried out after the mixture had cured in air for 48 hours. The 48-hour curing time was sufficient to allow the slow-acting hydrated lime to modify the properties of the soil.

(i) Particle Size Analysis

The percentage distribution of solid grains according to their dimensions is proportional to the size of the particles. Two types of tests are carried out to separate the particles: sieving after 48 hours of curing the soil-lime mixture in air for grains of size $\phi > 80$ µm in accordance with standard NF P94-056 [12] and sedimentation for grains of diameter $\phi \leq 80$ µm according to NF P94-057 [13]. The grain size fraction is deduced from the grain size nomograms of the recommendations, considering clays as particles < 0.002 mm, silts 0.002-0.06 mm and sands 0.06-2 mm.

(ii) Dry Density

To determine the optimum moisture content OMC (%) for which compaction leads to a maximum dry density MDD (T/m^3), the normal Proctor test is used. For a material with pores, the more interactions there are between the particles, the better the cohesion of the soil. The optimum moisture content and maximum dry density were determined in accordance with standard NF P94-093 [14].

(iii) Linear Swelling

The CBR immersion index (I. CBRi) is measured after 4 days immersion in water. In this case, the test specimen is covered with overloads to hoop the surface of the sample and the linear swelling of the test specimen is measured. The linear swelling test is carried out in accordance with standard NF P94-078 [15].

(iv) Atterberg Limits

The plasticity index, liquidity limit (LL) and plasticity limit (PL) were determined in accordance with standard NF P94-051 [16].

(v) Hydraulic Conductivity

The laboratory permeameter is used to measure the hydraulic saturation conductivity of undisturbed soil samples in sampling rings is in accordance with the NF EN ISO17892-11 [17], standard. The standard specifies the methods for the laboratory determination of the water circulation characteristics in soil. It applies to the laboratory determination of the permeability coefficient of soil in the context of geotechnical investigations. The coefficient of permeability (K-factor) gives precise information on:

- The presence of soil horizons that may prevent a rapid evacuation of a flow of precipitation water into the soil;
- The correlation between permeability and other geotechnical properties of the soil;
- Vertical and horizontal permeability (diffusion).

Figure 4 shows the apparatus (permeameter) used in the laboratory to measure the hydraulic conductivity of natural soil and soil-lime mixtures.

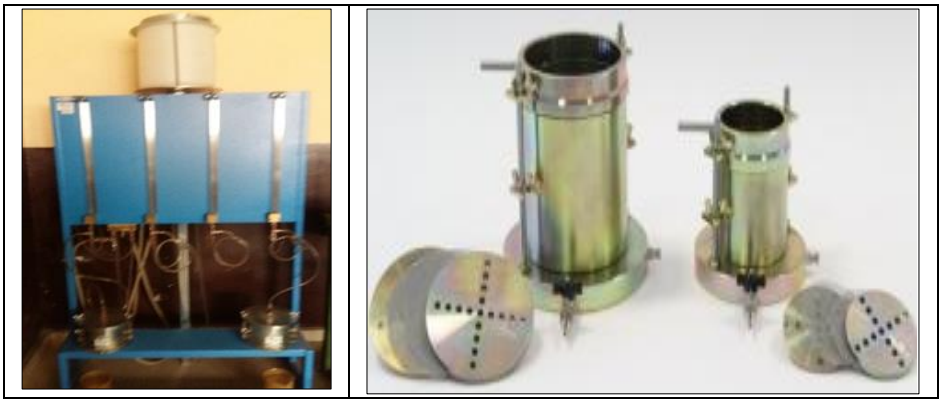

Fig. 4: Equipment for ksat testing using PPR and moulds for compacting the material NF X 30-441, [18]

Figure 4 shows that after compaction using Proctor Normal energy in accordance with standard NF P 94-093 [14], the specimen is saturated. The entire specimen plus the cell with the valves open is immersed in a water chamber (under a vacuum of up to 70 kPa) for 48 hours. After the saturation phase, the valves are closed and the cell is mounted on the test bench. In the next phase, the water is circulated in the test tube by applying a hydraulic head difference between its two surfaces for a time t. The hydraulic load is measured using a graduated tank tube. As in the variable-load permeability test with the oedometer, the curve of change in hydraulic load $\ln(h_1/h_2)$ as a function of time t is established (h_1 is the hydraulic load at the start of the permeability measurement phase, h_2 is the hydraulic load at time t). On the linear part of the curve, the saturated permeability of the soil is determined on the basis of Darcy's law according to the equation below:

$$K = \frac{a\,x\,l}{A\,x\,t}\,x\,ln\frac{h_1}{h_2} \qquad (1)$$

a (m^2) - cross-sectional area of the piezometer tube;
l (m) - height of the test piece during the permeability measurement phase;
A (m^2) - cross-sectional area of the test piece;
t (s) - time interval between two consecutive measurements.

Phillips XL30 EM scanning electron microscopy (SEM) provides information on the relief of the sample, grain morphology, and grain arrangement in the material.

Figure 5 shows an overview of the laboratory study of the hydraulic conductivity of natural soil and soil-lime mixtures.

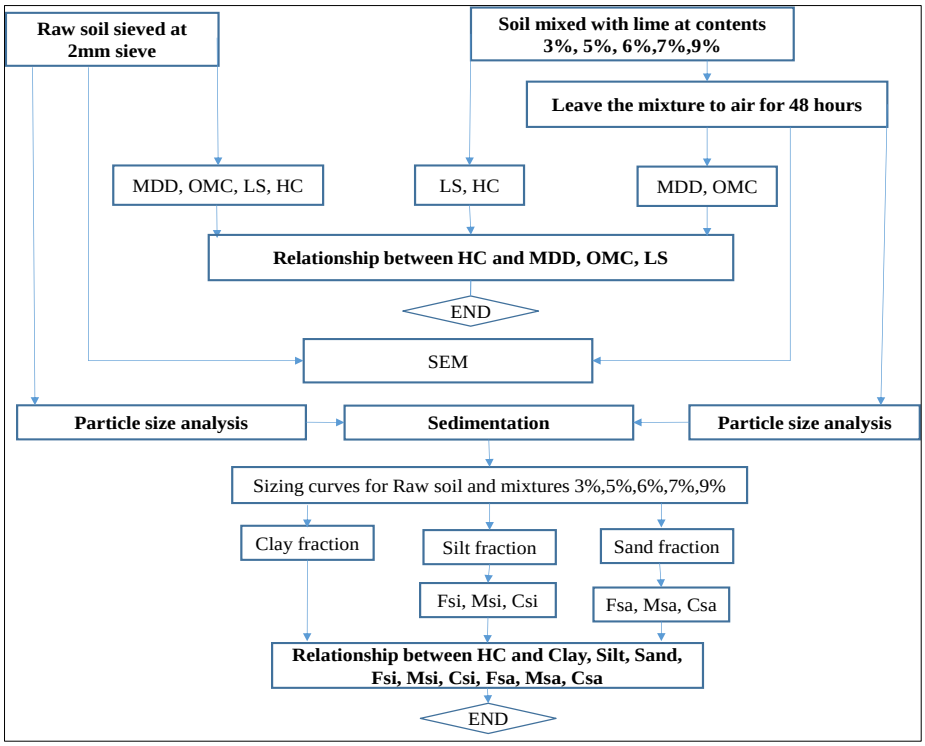

Fig. 5: Flow chart of laboratory tests

The symbols in Figure 5 can be explained as follows: MDD – maximum dry density, OMC – optimum moisture content, SEM – scanning electron microscopy, HC - hydraulic conductivity, LS - linear swelling, Fsi - fine silt, Msi – medium silt, Csi – coarse silt, Fsa – fine sand, Msa – medium sand, Csa – coarse sand.

The protocol for carrying out the laboratory tests indicates that after the material has been sieved in the laboratory, the following tests are carried out on the raw soil: granulometric analysis to determine the granulometric fractions (clay, silt, sand), normal Proctor, linear swelling and hydraulic conductivity. Relationships between geotechnical properties and hydraulic conductivity were established for the raw soil. Then, for the soil-lime mixtures, the mixtures was left in the open air for 48 hours, to allow the lime to attack the fine clayey and modify the particle size in the mixtures. The mixtures were identified and the particle size fractions extracted from the particle size curves, and correlations between the geotechnical properties of the mixtures and the hydraulic conductivity were established.

3. RESULTS

3.1 *Geotechnical Properties of Lime Treated Cubitermes Sp Termite Mound Soil*

Figure 6 shows the particle size distribution of the raw soil and that of the soil-lime mixtures obtained after a curing period.

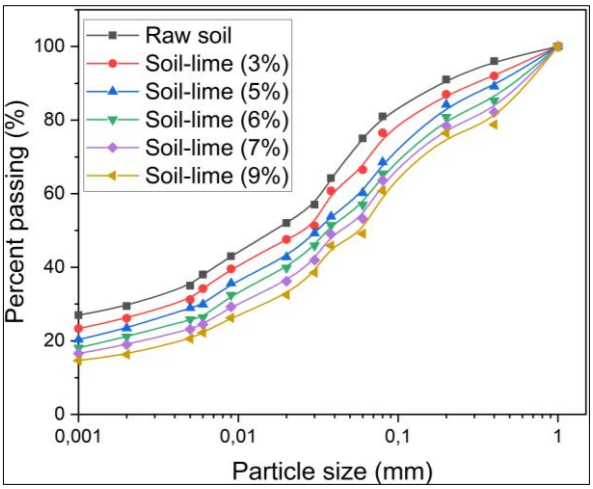

Fig. 6: Sieve size curves for raw soil and soil-lime mixtures

Figure 6 shows the particle size distribution of the raw soil and the soil-lime mixtures. The 48-hour curing time modified the particle size distribution of the soil-lime mixtures. The particle size fractions are deduced from Figure 6 in accordance with the particle size nomograms in the recommendations, considering coarse sand = Csa (0.63 – 2 mm); medium sand = Msa (0.2 - 0.63 mm) ; fine sand = Fsa (0.063 - 0.2 mm) ; coarse silt = Csi (0.02 - 0.063 mm) ; medium silt = Msi (0.0063 - 0.02 mm) ; fine silt = Fsi (0.002 - 0.0063 mm) ; clay fraction = CF (< 0.002 mm). The clay, silt (fine, medium, coarse) and sand (fine, medium, coarse) contents of this raw soil and of the mixtures extracted from Figure 6 are given in Table 1.

Table 1: The grain size fractions of natural soil and mixtures

Lime (%)	Particle size fractions (%)								
	CF	SiF	Fsi	Msi	Csi	SaF	Fsa	Msa	Csa
0	29.45	45.12	8.89	13.28	22.95	25.43	15.79	7.35	2.29
3	26.14	40.39	7.49	12.86	20.04	33.47	19.72	9.19	4.56
5	23.45	36.98	6.58	12.62	17.78	39.57	22.39	10.89	6.29
6	21.14	36.28	6.41	12.48	17.39	42.58	22.65	11.91	8.02
7	18.78	35.4	6.32	11.94	17.14	45.82	23.18	13.47	9.17
9	16.29	33.55	6	10.57	16.98	50.16	24.36	14.62	11.18

Table 1 explains that the lime content of (0%) represents the raw soil and explains symbols such as: CF – clay fraction, SiF – silt fraction, SaF – sand fraction, Fsi – fine silt, Msi – medium silt, Csi – coarse silt, Fsa – fine sand, Msa – medium sand, Csa – coarse sand.

Table 1 shows that all the changes in particle size occur after the consolidation of the grains by flocculation, which modifies the nature of the raw soil. In other words, the addition of lime modified the initial granulometry of the natural soil through the formation of aggregates, thus improving the useful properties of the treated soil [8, 9].

Table 2 shows the results obtained after laboratory tests on permeability, linear swelling and the optimum moisture content required to obtain maximum compaction energy from the raw soil and the soil-lime mixture.

Table 2: Geotechnical properties of cubitermes sp termite mound soil.

Lime (%)	K (cm/s)	LS (%)	MDD (T/m^3)	OMC (%)
0 %	1.3510^{-9}	3.4	1.62	20
3 %	7.8810^{-8}	2.7	1.6	21.28
5 %	6.4410^{-7}	1.98	1.55	22.06
6 %	6.4810^{-7}	1.69	1.5	22.92
7 %	5.810^{-7}	1.2	1.458	23.85
9 %	5.5810^{-7}	0.8	1.36	24.79

The symbols in Table 2 can be explained as follows: K – drainage coefficient, MDD – Maximum dry density, OMC – Optimum moisture content, LS – Linear Swelling.

Table 3 shows the classification of the raw soil and the evolution of the classification of soil-lime mixtures based on the AASHTO and USCS international soil classifications.

Table 3: Classification of raw soil and lime-soil mixtures

LC	P (0.075 mm)	LL	PL	PI	Classification	
(%)					AASHTO	USCS
0 %	41.49	36.20	18.44	17.76	A-6	Clayey silt
3 %	37	35.75	18.83	16.92	A-6	Sandy silt
5 %	33.55	35.55	18.95	16.6	A-2-6	Silty sand
6 %	29.85	35.44	19.06	16.38	A-2-6	Silty sand
7 %	26.96	35.4	19.10	16.3	A-2-6	Silty sand
9 %	24.28	35.25	19.15	16.1	A-2-6	Silty sand

The symbols in Table 3 can be explained as follows: P - 0.075 mm sieve pass, LL – liquidity limit, PL – plasticity limit, PI – plasticity index, AASHTO - American Association of State Highway and Transportation Officials [10], USCS - Unified Soil Classification System [11].

Figure 7A shows the evolution of the compaction energy as a function of the moisture content and Figure 7B shows the evolution of the maximum compaction energy as a function of the optimum moisture content of the raw soil and the soil-lime mixtures.

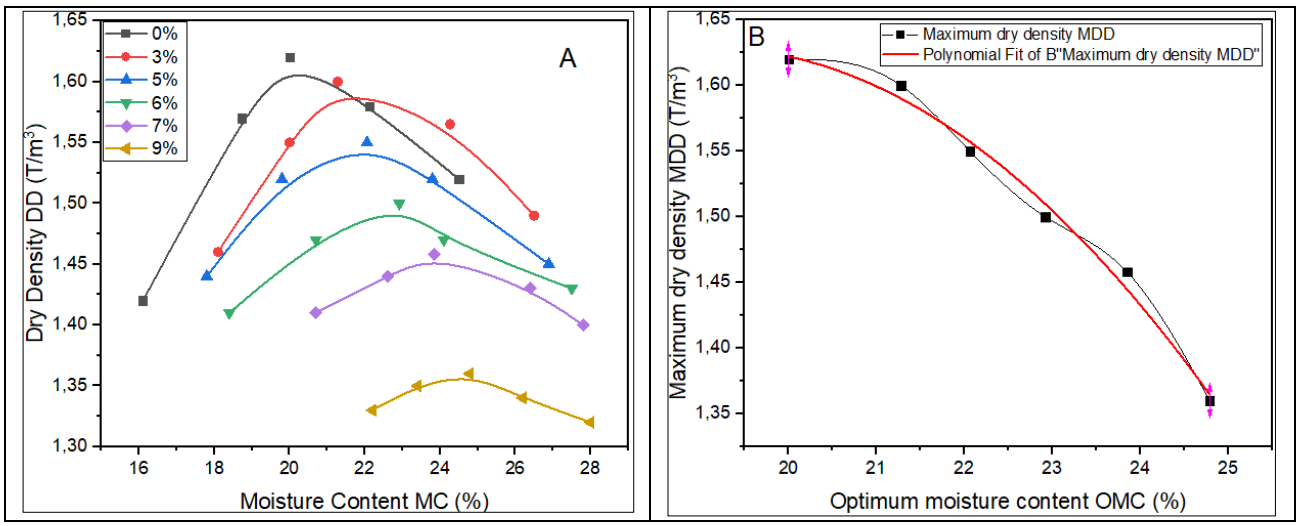

Fig. 7: Relationship between dry density and moisture content (%)

The evolution of the decrease in maximum dry density (Figure 7B) as a function of optimum moisture content is a polylinear fit:

$$Y_1 = C + AX + BX^2 \quad (2)$$

$$MDD = C + A(OMC) + B(OMC)^2 \quad (3)$$

Table 4 shows the values of the constants A, B and C of polylinear fit (3), obtained after correlation between maximum dry density and optimum moisture content.

Table 4: Determination of the constants C, A, B and R^2 of polylinear fit (3)

Y_1	C	A	B	R^2
MDD	-1.358 ± 1.063	0.313 ± 0.095	-0.008 ± 0.002	0.984

The symbols in Table 3 can be explained as follows: MDD (T/m^3) – maximum dry density, OMC (%) - optimum moisture content, R^2 - coefficient of determination. Figures 7A and 7B show that the dry density (compaction energy of the material) decreases with the addition of lime, which increases the sand content by 97.25% (Table 1). The Proctor curves shift to the right towards the higher water contents, due to the pozzolanic soil-lime reaction. The modified Proctor curves eventually flatten out as the sand content increases (Table 1). The addition of lime (0-9%) increases the optimum moisture content by 23.95% (Table 2) and coarse sand by 388.21% (Table 1), resulting in a decrease in compaction energy from 1.62 T/m^3 to 1.36 T/m^3 (Table 2) [9-20]. Figure 8 shows the evolution of hydraulic conductivity as a function of the added lime content and the water saturation time of the raw soil and the soil-lime mixture. Figure 8 also shows that the saturation time of the raw soil sample is much higher than that of the mixtures because the raw soil was impermeable. However, as lime is hydrophilic, its addition accelerates water saturation of the sample while reducing its saturation time.

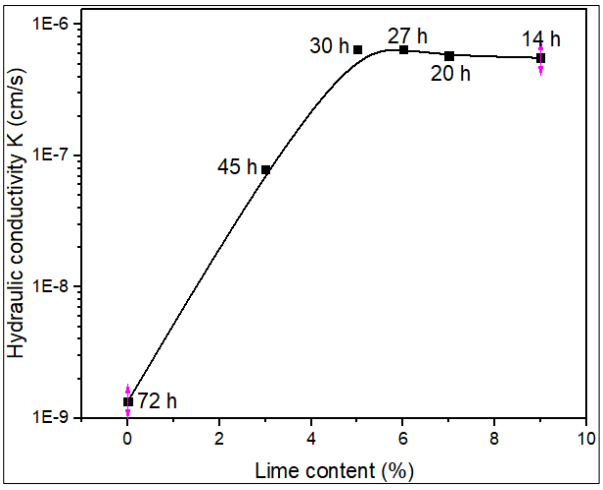

Fig. 8: Changes in hydraulic conductivity of intact (reconstituted) soil samples as a function of lime addition and saturation time

The drainage coefficient of raw soil is K (10^{-9} cm/s), which is at the upper limit of practically impermeable soils such as unweathered homogeneous clays or clayey silts. Soil-lime mixtures at 3%, 5%, 6%, 7% and 9% have a drainage coefficient K (10^{-8} - 10^{-7} cm/s), consisting of very fine sands, silts and sand-lime-clay mixtures. These soils drain poorly [7]. This result is in accordance with the nature of the natural soil and mixtures studied. Indeed, according to the Taylor diagram for soil classification, based on the grain size fraction (clay, silt, sand), the natural soil of termite mounds is classified as clayey silt. Mixtures with 3%, 5%, 6% and 7% lime content are silt and mixtures with 9% lime content are sandy silt [10, 11].

Adding lime increases permeability up to a lime content of 6%, which corresponds to the lime fixing point (LFP). From 7 to 9% lime, permeability decreases slightly. Brandl (1981), McCallister (1990), Nalbantoglu and Tuncer (2001) [8-22], estimate that the permeability of lime-treated soil increases up to a certain amount of lime added, corresponding to the LFP. Above this quantity, permeability remains stable or even decreases. The increase in permeability follows the decrease in dry density resulting from the increase in sand content (sensitive to water) and the presence of pores in the soil. There is a reorganization of the particles induced by flocculation. In their research [8-23], believe that under given compaction energy, the maximum dry density of lime-treated soil is lower than that of natural soil, and therefore, the lower the dry density, the higher the hydraulic conductivity. Above 6% lime, i.e., at contents of 7% to 9%, the decrease of the maximum dry density is counterbalanced by the important precipitation of cementitious products reducing the water circulation in the soil and thus decreasing the permeability [8-22].

3.2 Correlations between Hydraulic Conductivity and Certain Geotechnical Soil Properties

Figure 9 shows the correlations obtained between hydraulic conductivity and the particle size fractions of clay, silt (fine, medium, coarse) and sand (fine, medium, coarse) in the raw soil and the soil-lime mixtures.

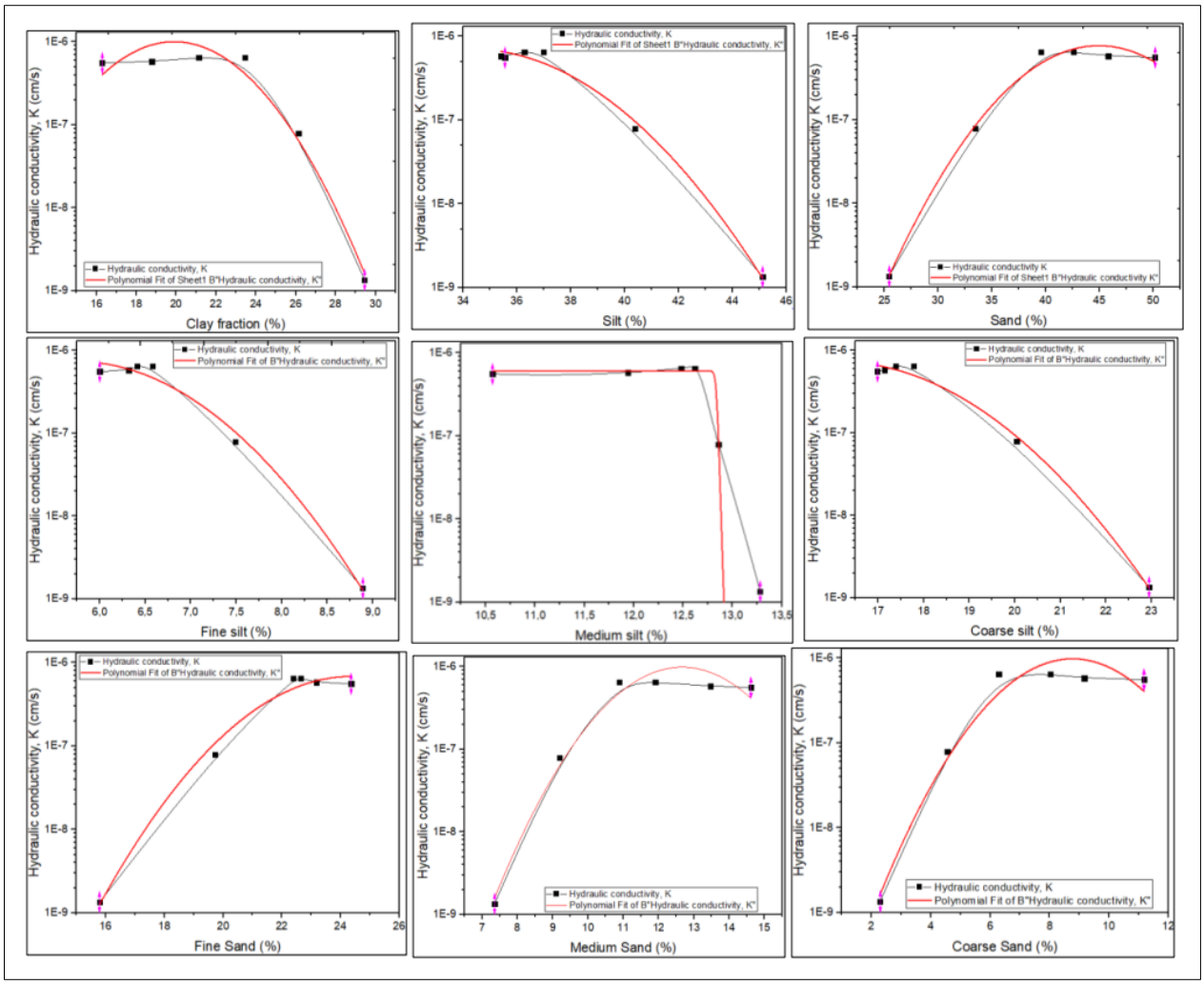

Fig. 9: Relationship between hydraulic conductivity and particle size fractions of raw soil and soil-lime mixtures

Figure 9 shows that hydraulic conductivity is strongly correlated with particle size fractions. The evolution of hydraulic conductivity as a function of particle size fractions is a polylinear fit:

$$Y_2 = C + AX + BX^2 \quad (4)$$

$$HC = C + A(PSF) + B(PSF)^2 \quad (5)$$

With, PSF (%) – Particle size fraction, HC (cm/s) - hydraulic conductivity, R^2 - coefficient of determination.

Table 5 shows the constants A, B, C and R^2 of the polylinear fits (5) obtained after correlations between hydraulic conductivity and clay, silt (fine, coarse) and sand (fine, medium, coarse).

Table 5: Determination of the constants C, A, B and R^2 of polylinear fit (5)

PSF	C	A	B	R^2
Clay	-18.123 ± 2.493	1.219 ± 0.224	-0.031 ± 0.005	0.962
Silt	-33.719 ± 8.232	1.607 ± 0.413	-0.023 ± 0.005	0.989
Sand	-20.726 ± 1.007	0.650 ± 0.055	-0.007 ± 7.309E^{-4}	0.989
Fine silt	-15.276 ± 3.922	3.188 ± 1.069	-0.278 ± 0.071	0.986
Coarse silt	-21.308 ± 4.625	1.885 ± 0.471	-0.059 ± 0.012	0.993
Fine sand	-28.218 ± 3.063	1.81 ± 0.314	-0.037 ± 0.008	0.986
Medium sand	-21.855 ± 1.552	2.502 ± 0.292	-0.099 ± 0.013	0.974
Coarse sand	-21.308 ± 4.623	1.885 ± 0.471	-0.059 ± 0.012	0.993

Figure 9 also shows that the relationship between hydraulic conductivity and average silt fraction best fits the Slogistic1 model, with the following equation:

$$Y = \frac{a}{\left(1+exp\left(-k*(X-X_C)\right)\right)} \quad (6)$$

$$HC = \frac{a}{\left(1+exp\left(-k*(Msi-X_C)\right)\right)} \quad (7)$$

Table 6 shows the constants Y_0, X_0, A_1, t_1, R^2 and χ^2 of equation (7) of the Slogistic1 model obtained after correlation between hydraulic conductivity and average silt fraction.

Table 6: Determination of the constants Y_0, X_0, A_1, t_1, R^2 and χ^2 in the Slogistic1 model equation

Y	a	X_C	k	R^2	χ^2
HC	$6.075E^{-7}$±$2.621E^{-8}$	12.838±9628.295	-84.726 ± $3.631E^{-7}$	0.977	$2.06E^{-15}$

The symbols in table 6 and equation (7) are defined as follows: HC (cm/s) - hydraulic conductivity, Msi (%) – medium silt, R^2 - coefficient of determination, χ^2 - Chi-square is used to test the independence of two random variables.

Figure 10 shows the evolution of the coefficient of determination R^2 of the relationship between the hydraulic conductivity and the particle size fraction of the raw soil and the soil-lime mixtures.

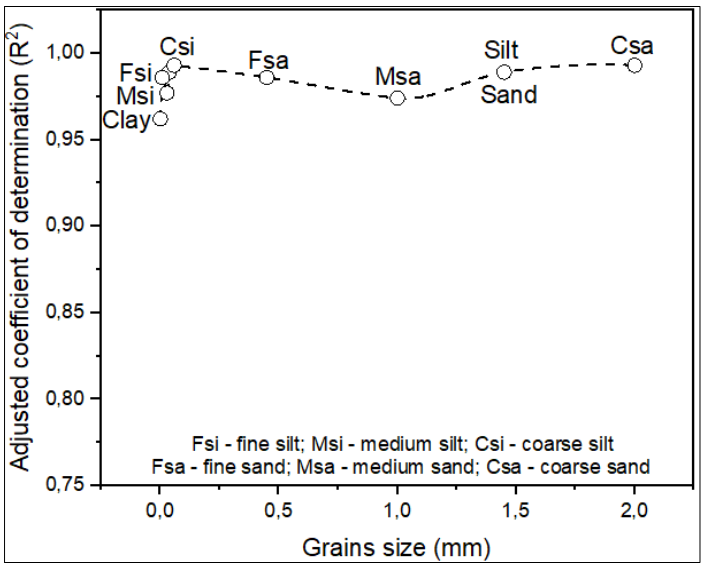

Fig. 10: Correlation between the adjusted coefficient of determination (R^2) as a function of grain size for raw soil and soil-lime mixtures

La variation du coefficient de détermination R2(0,962 - 0993) dans la figure 10 semble être liée au fait que le couple sol-chaux n'obéit pas à la loi du mélange.

Figure 11 shows the effect of the compaction energy of the raw soil and soil-lime mixtures on changes in hydraulic conductivity.

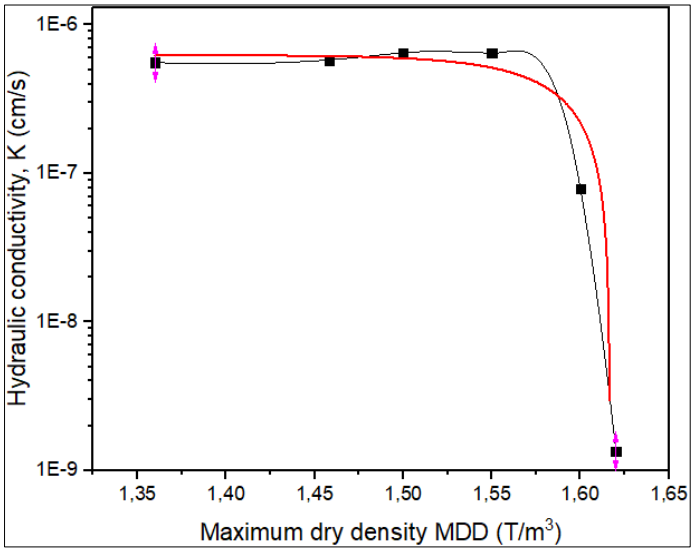

Fig. 11: Hydraulic conductivity as a function of maximum compaction energy

The evolution of hydraulic conductivity as a function of maximum compaction is fitted to the ExpGrow1 model equation:

$$Y = Y_0 + A_1 * exp\left(\frac{(X - X_0)}{t_1}\right) \quad (8)$$

$$HC = Y_0 + A_1 * exp\left(\frac{(MDD - X_0)}{t_1}\right) \quad (9)$$

Table 7 shows the values of the constants in [9] and the coefficients R^2, χ^2 obtained from the correlation between the hydraulic conductivity as a function of the maximum compaction energy of the raw soil and the soil-lime mixtures.

Table 7: Determination of the constants Y_0, X_0, A_1, t_1, R^2 and χ^2 in the ExpGrow1 model equation [9]

Y	Y_0	X_0	A_1	t_1	R^2	χ^2
HC	$6.26E^{-7} \pm 1.077E^{-7}$	1.095±394993.46	$-8.54E^{-13} \pm 8.73E^{-6}$	0.039±0.028	0.724	$2.42E^{-14}$

With, HC (cm/s) - hydraulic conductivity, MDD (T/m^3) – maximum dry density, R^2 - coefficient of determination, χ^2 - Chi-square is used to test the independence of two random variables.

Figure 12 shows the evolution of the hydraulic conductivity of the raw soil and the soil-lime mixtures, when the material is compacted to the optimum moisture content of the normal Proctor test.

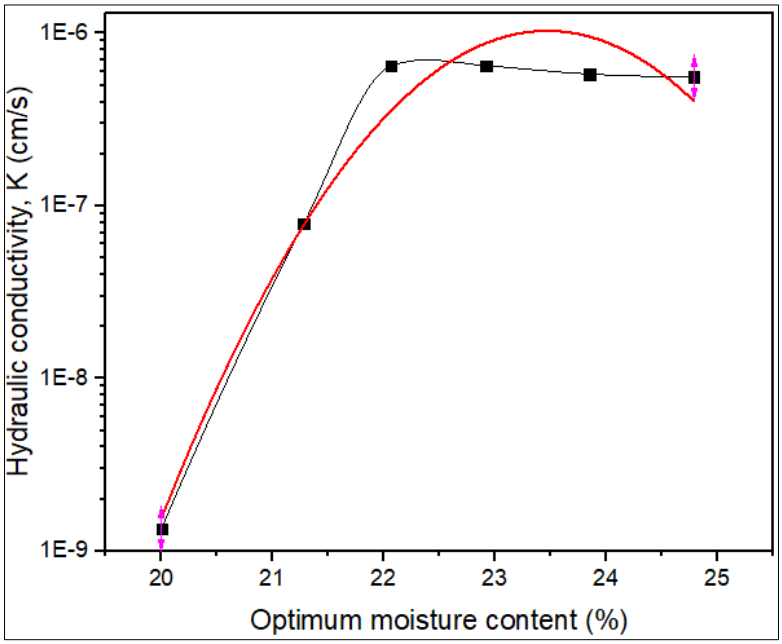

Fig. 12: Hydraulic conductivity as a function of optimum moisture content

The evolution of hydraulic conductivity as a function of optimum moisture content is a polylinear fit:

$$Y_3 = C + AX + BX^2 \quad (10)$$

$$HC = C + A(OMC) + B(OMC)^2 \quad (11)$$

Table 8 shows the values of the constants in [11], and the coefficient R^2 obtained from the correlation between the hydraulic conductivity as a function of the optimum moisture content of the raw soil and the soil-lime mixtures.

Table 8: Determination of the constants C, A, B and R^2 of polylinear fit [11]

Y_3	C	A	B	R^2
HC	-135.059 ± 19.769	10.998 ± 1.770	-0.234 ± 0.039	0.955

With, HC (cm/s) – maximum dry density, OMC (%) - optimum moisture content, R^2 - coefficient of determination. Figure 13 shows the evolution of hydraulic conductivity as a function of linear swelling of the raw soil and the soil-lime mixtures.

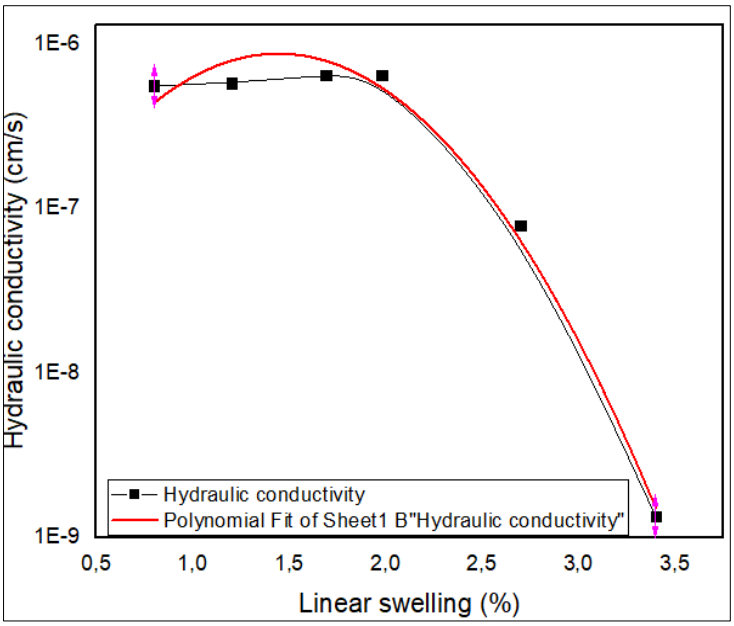

Fig. 13: Hydraulic conductivity as a function of linear swelling of compacted soil

Hydraulic conductivity as a function of linear swelling is a polylinear fit:

$$Y_4 = C + AX + BX^2 \quad (12)$$

$$HC = C + A(LS) + B(LS)^2 \quad (13)$$

Table 9 shows the values of the constants in [13], and the coefficient R^2 obtained from the correlation between the hydraulic conductivity as a function of the linear swelling of the raw soil and the soil-lime mixtures.

Table 9: Determination of the constants C, A, B and R^2 of polylinear fit [13]

Y_4	C	A	B	R^2
HC	-7.562 ± 0.321	2.082 ± 0.342	-0.721 ± 0.079	0.984

With, HC (cm/s) – conductivité hydraulique, LS (%) - linear swelling, R^2 - coefficient of determination.

3.3 Changes in Microstructure as a Function of Lime Addition

Figure 14 shows the changes observed in the microstructure of the raw soil after compaction at magnifications of 10 µm (A) and 5 µm (B).

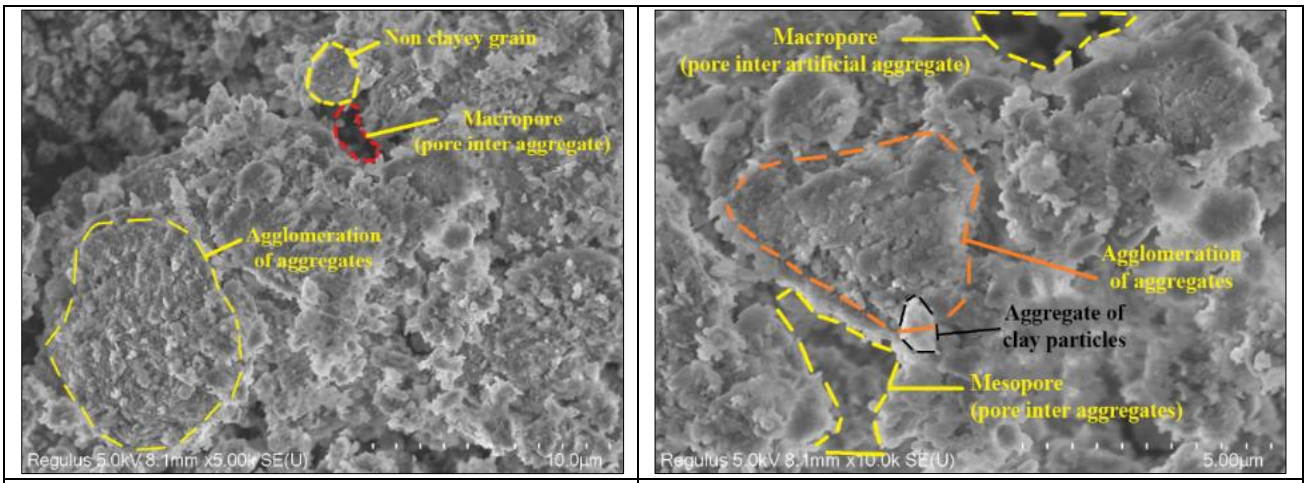

A) Magnification x 10 µm | **B) Magnification x 5 µm**

Fig. 14: A) Natural soil observation, magnification x 10 µm and B) magnification x 5 µm

Observation of the morphology of natural soil (Figure 14A) shows an internal structure composed of agglomerated grains and aggregates, sometimes dispersed and interspersed with macropores. Macropores are the artificial inter-aggregate pores resulting from compaction [24]. Figure 14B shows a soil structure made up of grains covered with aggregates, creating continuous bridges between the grains, between the

aggregates or between the aggregates and the grains. These aggregates are at the origin of the small mesopores that form the natural inter-aggregate pores [24].

The scanning electron microscope shows a soil with a bimodal pore distribution with a class of macropores and centred mesopores after the normal Proctor test. The results obtained show that the pore volume in the soil-lime mixtures is slightly greater than that of the corresponding natural soil. In other words, the compaction energy decreases as the sand content in which the pores appear increases.

By observing the evolution of the normal Proctor curves (Figure 7A), the compaction of the soil-lime mixtures reveals a third family of very small pores (micropores) which appear after the fine sand content is increased (Table 1). This phenomenon occurs independently of the lime content. Macropores appear in the coarse sand, the content of which increases with the addition of lime (Table 1). In addition, it can be seen that, in parallel with the appearance of micropores in the fine sand, the quantity of macropores in the coarse sand decreases sharply in the soil-lime mixture compared with the natural soil. Figure 15 shows the changes observed in the microstructure of the 3% soil-lime mixture after compaction.

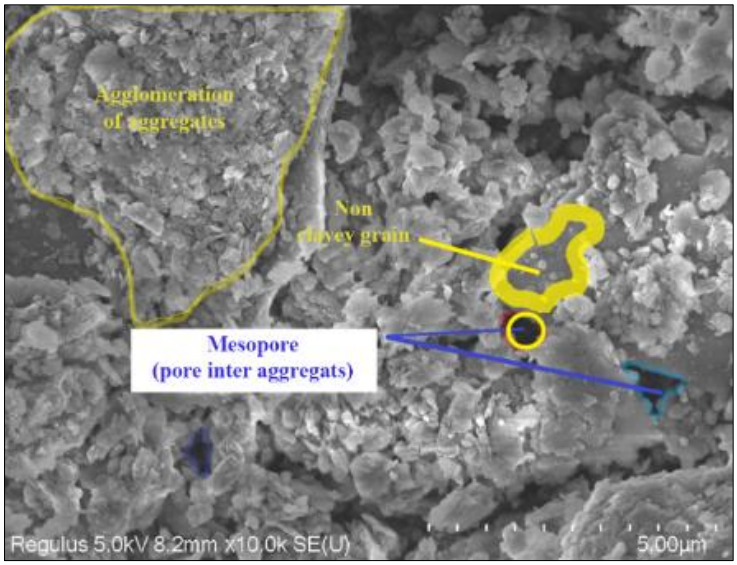

Fig. 15: Morphology of soil treated with 3% lime, magnification x 5 µm

The morphology of the soil treated with 3% lime (Figure 15), compared with that of the natural soil (Figure 14A) observed at the same magnification, shows a treated soil with a denser internal structure with agglomerations of aggregates and dispersed aggregations of clay particles. The aggregate agglomerations fill the artificial inter-aggregate macropores and reduce the pore volume. Figure 16 shows the changes observed in the microstructure of the 6% soil-lime mixture after compaction.

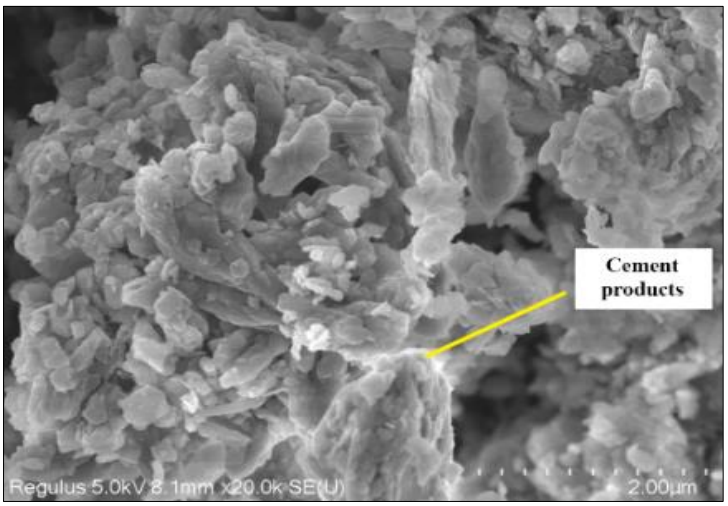

Fig. 16: Morphology of soil treated with 6% lime, magnification x 2 µm

Figure 16 shows the morphology of a soil treated with 6% lime. The texture of the soil does not allow clay minerals to be observed at the surface of the grains. However, the new minerals formed at the surface of the grains are cementitious products (C-S-H or C-A-S-H) created by pozzolanic reactions. The new products fill the mesopores (the natural pores between aggregates) present in the medium sand.

Figure 17 shows the changes observed in the microstructure of the 7% soil-lime mixture after compaction.

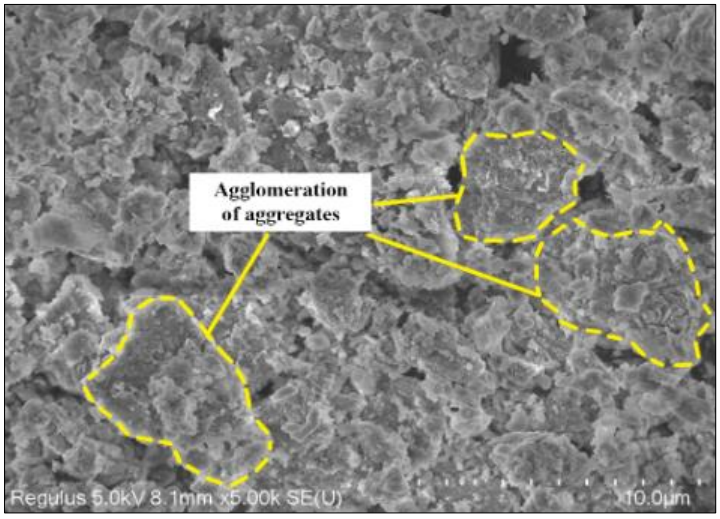

Fig. 17: Morphology of soil treated with 7% lime, magnification x 10 µm

Compaction to reduce pores in treated soil is greater than in natural soil. Compaction is correlated with the lime dosage and the curing time. Figure 18 shows the changes observed in the microstructure of the 9% soil-lime mixture after compaction.

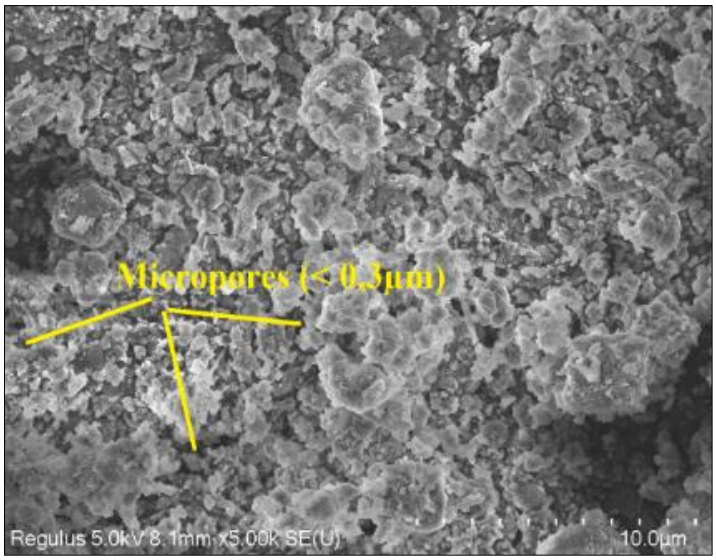

Fig. 18: Morphology of soil treated with 9% lime, magnification x 10 µm

The evolution of the void index reduces the mechanical performance of the material. Increasing the lime content reduces compaction energy. Acar and Oliveri (1989) also showed that increasing the compaction force decreases the frequency of large pores and can eliminate the mode of large pores. The development of cementitious binders formed during pozzolanic reactions modifies the microstructure of the mixture.

3.4. DISCUSSION

Table 1 shows the changes in the size fractions of clay, silt (fine, medium, coarse) and sand (fine, medium, coarse). The addition of 0-6% lime changes the particle size fraction by reducing the clay and silt fractions by 28.22% and 19.59% respectively, and the sand content increases by 67.44%. Fine, medium and coarse silts decreased by 27.90%, 6.02% and 24.23%, respectively. Fine, medium and coarse sands increased by 43.45%, 62.04% and 250.22% respectively. In the 6-

9% lime content range, clay and silt contents fall by 22.94% and 7.52% respectively. Fine, medium and coarse silts decreased by 6.40%, 15.30% and 2.36%, respectively. Fine, medium and coarse sands increased by 7.55%, 22.75% and 39.40% respectively. The decrease in clay and silt fractions and the increase in sand fractions are significant when the lime content is between 0 - 6% and lower when the lime content is between 6 - 9%. A lime content of 6% is considered the fixing point for lime (FPL).

From tables 2 and 3, the raw soil is a class A-6 clayey silt whose coefficient of permeability obtained after 72 h of K (1.3510^{-9} cm/s) is less than 10^{-7} cm/s, i.e., the soil is practically impermeable [7]. The mixture with 3% lime is a class A-6 sandy silt with a coefficient of permeability obtained after 45 h of K (7.8810^{-8} cm/s), lower than 10^{-7} cm/s, the soil is practically impermeable [7]. Mixtures with 5-9% lime are class A-2-6 silty sands, with permeability coefficients obtained between 30-14 h (Figure 8) of K (6.4410^{-7} - 5.5810^{-7} cm/s), i.e., these mixtures have poor drainage [7]. Impermeable soils and those with poor drainage are favorable for the execution of civil engineering works (earthworks) [7]. Lime is hydrophilic (absorbs water), and this property is widely used in civil engineering to dry out wet soils.

In Figure 7, increasing the sand fraction with the addition of lime reduces the maximum dry density, causing the Proctor curves to flatten and shift towards the higher moisture content. Although the Proctor test is mainly used to determine the water content required to obtain maximum dry density, the fact remains that for a given material, the fewer pores there are, the more interaction there is between the different particles and, in principle, the more cohesion there is.

The increase in permeability (Figure 8) depends on the increase in the sand fraction of the mixtures (Table 1), with the appearance of micropores in fine sands, mesopores in medium sands and macropores in coarse sands. The increases in permeability and sand fraction are all linked to the addition of lime up to a content of 6%. From 7 to 9% lime content, permeability decreases slightly, while the sand fraction continues to increase. The 6% lime content can be considered the lime fixation point (LFP). Above 6% lime, there is a reorganisation of the microstructure manifested by a strong agglomeration of soil grains (Figure 17). Brandl (1981), McCallister (1990), Nalbantoglu and Tuncer (2001) [8-22], estimate that the permeability of a lime-treated soil increases up to a certain quantity of lime added, corresponding to the lime fixation point. Above this quantity, permeability remains stable or even decreases.

Figure 9 and Tables 5 and 6 provide correlations for the prediction of soil hydraulic conductivity as a function of sand fractions with R^2 (0.962 - 0.993) (Figure 10) and χ^2 ($2.06E^{-15}$) for medium silt. Figure 11 shows the relationship used to predict hydraulic conductivity as a function of the decrease in compaction energy resulting from the increase in the sand fraction. The coefficient of determination R^2(0.724) is linked to the soil-lime mixture, which does not obey the law of mixtures [26]. Observation of the morphology of raw soil (Figure 14) shows an internal structure composed of agglomerated grains and aggregates, sometimes dispersed and interspersed with macropores. Macropores are artificial inter-aggregate pores resulting from the reduction in compaction energy following the increase in the sand fraction.

According to Figure 16, the pore volume of the soil treated with 6% lime is lower than that of the raw soil, due to the formation of cementitious products that fill the mesopores and macropores present in the medium and coarse sands respectively.

According to Figure 17, the effect of lime treatment on soil microstructure reveals three families of pores defined as follows: micropores in fine sand (0.0072 - 0.3 µm), mesopores in medium sand (0.3 - 6 µm), macropores in coarse sand (> 6 µm). According to Figure 15-18, the elimination of pores in the microstructure is achieved by increasing the mould water content above the optimum water content and the compaction energy, which reduces the permeability and load-bearing capacity of the soil [6-28].

4. CONCLUSION

This work examines the relationship between geotechnical properties and microstructure to explain the hydraulic conductivity of a cubitermes sp termite mound soil treated with lime. The results obtained show significant changes in granulometry, manifested by a decrease in the clay and silt fraction, offset by an increase in the sand content. The changes in particle size are partly responsible for the decrease in dry density, plasticity index, linear swelling, increase in permeability and optimum water content. The multitude of changes in soil properties can be explained by the interaction of the underlying microstructural mechanisms during the pozzolanic reactions. The pore volume of the treated soil samples is slightly larger than that of the natural soil sample due to the decrease in the compaction energy of the material caused by the increase in the sand fraction. The microstructure of soil-lime mixtures evolves in the same way as that of natural soil. The permeability of the soil decreases with increasing water content and compaction energy, leading to closure of the microstructure. For lime contents of 7 to 9%, the decrease in maximum dry density is counterbalanced by the high precipitation of cementitious products, which reduces the circulation of water in the soil and therefore decreases permeability. The saturation time of the water in the mixture decreases with the addition of lime. Correlations for the prediction of soil hydraulic conductivity as a function of particle size fractions are polylinear fits with R^2(0.962 - 0.993) and χ^2 ($2.06E^{-15}$) for medium silt. Correlations between permeability and

compaction energy is an ExpGrow1 model fit with R^2(0.724) and χ^2(2.42E^{-14}). Correlations between permeability as a function of linear swelling and optimum water content is a linear fit with R^2(0.955 - 0.984). Hydraulic conductivity is strongly correlated with the increase in coarse sand with R^2(0.993).

Declarations

Conflict of Interest: The authors declare no competing interests

5. REFERENCES

1. Elenga, R. G., Ahouet, L., Ngoulou, M., Bouyila, S., Dirras, G. F., & Kengué, E. (2019). Improvement of an Alluvial Gravel Geotechnical Properties with a Clayey Soil for the Road Construction. *Research Journal of Applied Sciences, Engineering and Technology*, *4*, 135-139. https://doi: 10.19026/rjaset.16.6017.
2. Loubouth, S. J. M., Ahouet, L., Elenga, R. G., Okina, S. N., & Kimbembe, P. L. (2020). Improvement of the Geotechnical Properties of the Soil of Lime-Treated Cubitermes Mound Soil. *Open Journal of Civil Engineering*, *10*(01), 22. https://doi.org/10.4236/ojce.2020.101003.
3. AHOUET, L., & ELENGA, R. G. (2019). Amélioration des propriétés géotechniques du graveleux latéritique par ajout de la grave alluvionnaire concassée 0/31, 5. *Sciences Appliquées et de l'Ingénieur*, *3*(1), 1-6.
4. Savage, P. F. (2007). Evaluation of Possible Swelling Potential of Soil. Proceedings of the 26thSouthern African Transport Conference (SATC 2007). ISBN: 1-920-01702-X.
5. Lemaire, K., Deneele, D., Bonnet, S., & Legret, M. (2013). Effects of lime and cement treatment on the physicochemical, microstructural and mechanical characteristics of a plastic silt. *Engineering Geology*, *166*, 255-261. https://doi.org/10.1016/j.enggeo.2013.09.012.
6. Acar, Y. B., & Olivieri, I. (1989). Pore fluid effects on the fabric and hydraulic conductivity of laboratory-compacted clay. *Transportation Research Record*, (1219). http://worldcat.org/isbn/030904815X.
7. Terzaghi,K., Peck, R. B., & Mesri, G. (1996). Third Edition. Soil Mechanics in Engineering Practice. books.google.com.
8. Brandl, H. (1981). Alteration of soil parameters by stabilization with lime. Actes de la 10eme Conférence Internationale sur la mécanique des sols et les fondations Stockholm, Suede, 587-594. trid.trb.org.
9. Kavak, A., & Akyarlı, A. (2007). A field application for lime stabilization. *Environmental geology*, *51*, 987-997. Doi: 10.1007/s00254-006-0368-0.
10. AASHTO T88-70. The American Association of State Highway and Transportation Officials system is used worldwide for road construction.
11. Unified Soil Classification System (USCS). This system is applicable to projects such as dams, foundations and runways. The basic principle of this system is to classify coarse-grained soils according to their grain size and fine-grained soils according to their plasticity.
12. NF P 94-056 (1996). French Standard. Soils: Recognition and Tests. Granulometric Analysis. Method by Dry Sieving after Washing, French Standards Association, 5-15.
13. NF P94-057 (1992). French Standard. Soils: Recognition and Tests. Granulometric Analysis. Sedimentation Method, French Standards Association, 4-17.
14. NF P 94-093 (2014). French Standard. Soils: reconnaissance and testing - Determining the compaction references of a material - Normal Proctor test - Modified Proctor test.
15. NF P 94-078 (1997). French Standard: Soils: Reconnaissance and tests - CBR index after immersion - Immediate CBR index - Immediate bearing index - Measurement on compacted sample in the CBR mould.
16. NF P94-051 (1993). French Standard. Soils: Recognition and Tests. Determination of Atterberg Limits. Limit of Liquidity at the Cup Limit of Plasticity at the Roller. French Standards Association, 4-14.
17. NF EN ISO17892-11 (2019). French Standard: Geotechnical investigation and testing - Laboratory tests on soils - Part 11: Permeability tests. Afnor EDITIONS. https://www.boutique.afnor.org .
18. NF X 30-441 (2008). French Standard: Waste - Laboratory determination of the saturation permeability coefficient of a material - Permeability tests using a rigid wall permeameter with a constant/variable hydraulic gradient. Afnor EDITIONS. https://www.boutique.afnor.org.
19. Bell, F. G. (1996). Lime Stabilization of Clay Minerals and Soils. *Engineering Geology*, *42*(4), 223-237. https://doi.org/10.1016/0013-7952(96)00028-2.
20. Mtallib, M. O. A., & Bankole, G. M. (2011). Improvement of Index Properties and Compaction Characteristics of Lime Stabilized Tropical Lateritic Clays with Rice Husk Ash(RHA) Admixtures. *Electronic Journal of Geotechnical Engineering*, *16*.
21. McCallister, L. D. (1990). *The effects of leaching on lime-treated expansive clays*. The University of Texas at Arlington.
22. Nalbantoglu, Z., & Tuncer, E. R. (2001). Compressibility and hydraulic conductivity of a chemically treated expansive clay. *Canadian geotechnical journal*, *38*(1), 154-160.
23. Rajasekaran, G., & Rao, S. N. (2002). Permeability characteristics of lime treated marine clay. *Ocean engineering*, *29*(2), 113-127. https://doi.org/10.1016/S0029-8018(01)00017-8.
24. Tran, T. D. (2014). Role of the microstructure of clay soils in shrinkage and swelling processes: from the specimen scale to the environmental chamber

scale. Paris: Thesis Doctoral School no. 398: Geosciences, Natural Resources and Environment. HAL-Pastel. https://pastel.hal.science › docid › 2014ENMP0002.

25. Benson, C. H., Zhai, H., & Wang, X. (1994). Estimating hydraulic conductivity of compacted clay liners. *Journal of geotechnical engineering*, *120*(2), 366-387.
26. Ahouet, L., Okina, S. N., & Ekockaut, J. A. B. (2023). Effect of lime addition on the particle size fractions and microstructure of a clayey silt. *Arabian Journal of Geosciences*, *16*(10), 548. https://doi.org/10.1007/s12517-023-11625-5.
27. Le Runigo, B. (2008). *Durabilité du limon de Jossigny traité à la chaux et soumis à différentes sollicitations hydriques: comportements hydraulique, microstructural et mécanique* (Doctoral dissertation, Ecole Centrale de Nantes (ECN)/Université de Nantes).
28. Garcia-Bengochea, I., Altschaeffl, A. G., & Lovell, C. W. (1979). Pore distribution and permeability of silty clays. *Journal of the geotechnical engineering division*, *105*(7), 839-856.